Fermilab FERMILAB-Pub-02/043-E-REV October 2002

ASSESSMENT OF THE PROMPT RADIATION HAZARDS OF TRAPPED ANTIPROTONS

J. Donald Cossairt and Nikolai V. Mokhov*

Abstract - Investigators at several laboratories are seriously considering the storage and transport, perhaps over long distances, of very low energy antiprotons as a part of basic physics research programs and perhaps even for practical applications. To do this will require proper attention to the prompt radiation hazards due to the release of energy in the annihilations of antiprotons with nuclei, under either planned or accidental circumstances. In this paper, the potential storage of very low energy antiprotons is discussed and the major features of the radiation fields produced by their annihilations are reviewed both qualitatively and quantitatively. Detailed Monte Carlo Shielding calculations for a conceptual source of annihilating antiprotons nearly at rest are presented. It is concluded that these radiation fields are readily understood and that the radiation hazards can be mitigated using conventional means.

Key words: antiprotons, dose assessment, hadrons, photons, shielding, Monte Carlo calculations

*Fermi National Accelerator Laboratory, P. O. Box 500, Batavia, IL 60510. For correspondence of reprints contact J. Donald Cossairt at the above address or email at cossairt@fnal.gov.

INTRODUCTION

The antiproton, the antiparticle of the ordinary proton, has now been studied for over 40 years (Eades and Hartmann 1999). Over the last two decades, a number of investigators have speculated on the possibility that these particles can be stored at low kinetic energy and perhaps even transported. Antiprotons of relatively high energies have been copiously produced at the proton accelerators at both the European Organization for Nuclear Research (CERN) in Geneva, Switzerland and the Fermi National Accelerator Laboratory (Fermilab) in Batavia, IL, USA using proton-nucleus interactions at high energies. At both of these laboratories, the principal disposition of these particles has been their collection in storage rings followed by their subsequent acceleration to high energies for collision with protons in particle physics experiments conducted at frontier energies on the TeV-scale of 10^{12} electron volts. Other important basic research studies with antiprotons have been conducted at more modest energies; for example, the body of work performed at the low-energy antiproton ring (LEAR) at CERN where antiprotons having low momenta are acquired by decelerating higher energy antiprotons. Review articles by Amsler and Myhrer (1991), Landau (1996), and Amsler (1998) provide useful summaries.

Since their invention in 1936, Penning traps have been used to store electrons, charged particles, and ions by means of special configurations of magnetic and electric fields designed to maintain stable orbits of these charged particles under conditions of high vacuum. Brown and Gabrielse (1986) have described these devices at length. Obviously, the trapping of antiprotons presents considerable technological challenges since the particles have to be produced, collected, and then stored. Antiprotons have been successfully captured in a Penning trap at very low energies at LEAR (Gabrielse et al. 1986). In this experiment, about 300 antiprotons were

captured and it was concluded that confinement of perhaps 30,000 or so for time periods as long as 10 months is feasible. Currently, considerable effort is directed toward eventually studying cold antihydrogen in the laboratory (Gabrielse 2002). Howe, Hynes, and Picklesimer (1988) have investigated the research possibilities resulting from the ability to transport trapped antiprotons to locations distant from the large accelerators where they can be produced. The feasibility of the transport of as many as 10^{12} antiprotons in this manner was considered. The possibility of long distance transport has been demonstrated, in principle, by the successful shipment of electrons from California to Massachusetts in a Penning trap using a motor vehicle on highways (Tseng and Gabrielse 1993). Indicative of the near-term possibilities, this was achieved without connection to electrical power by using the persistent field of a superconducting magnet along with electric fields produced with 9 Volt batteries.

Practical Penning traps need not occupy large volumes. For example the trap discussed by Browne and Gabielse (1986) would fit in a 4 cm diameter sphere. Elsewhere, Gabrielse, et al. (1986) discusses a trap that would fit in a cylinder 2 cm diameter by 7 cm long.

Along with the obvious benefits to particle and nuclear physics, having antiprotons "readily available" at energies near rest in the laboratory frame of reference could be useful to the fields of atomic and condensed matter physics. There are also ideas that stored antiprotons might be useful as a compact source of stored energy perhaps in medicine or even in spaceflight. Thus, it behooves members of the radiation protection profession to understand further the associated radiological hazards in order to assist in the beneficial utilization of these particles. This topic has received little study since most interest in antiprotons has occurred at the high energy physics laboratories where they are produced. There, the radiation protection concerns involved with the proton-nucleus collisions used to produce the antiprotons generally dominate over those due to

the annihilating antiprotons.

METHODS

Radiation field produced by antiproton-nucleon annihilations

In this paper, those aspects of the radiation field emitted by antiproton-nucleon annihilations occurring at rest in the laboratory frame of reference that are important for radiation protection purposes will be emphasized, with the production of exotic particles and measurement of rare processes left to particle physics. At low energies near rest, the process of interest is solely that of annihilation. Pais (1960) employed group-theoretical techniques to describe the properties of systems of specific numbers of pions, working out various quantum numbers and branching ratios that are suitable for further use. The results were specifically applied to antiproton-nucleon annihilations and recognized that, "…the average number of π-mesons produced in $\bar{p}$- annihilation is about 5 or 6." Both charged ($\pi^{\pm}$) and neutral (π^{o}) pions are emitted from these events. Momentum conservation requires the emission of at least two particles from each annihilation event. Amsler (1998), in an up-to-date review paper, reported that average multiplicities in antiproton-proton annihilations at rest in the laboratory frame of reference are 3.0 ± 0.2 for charged pions and 2.0 ± 0.2 for neutral pions. Further, the numbers of pions are distributed statistically as a Gaussian function about these mean values, with a standard deviation of about one. The statistical model of antiproton annihilations has been called "the fireball model". Aside from pions, in antiproton-proton annihilations at rest the most prominent particles produced are the η-meson (rest energy of 547.3 MeV) in 7% of annihilations and the K-meson (rest energy of 493.7 MeV) in about 6%. All particle rest energies and mean lives used in this paper are those of the Particle Data Group (Groom et al. 2000).

For the situation of antiproton-proton annihilations occurring at rest, a simple statistical picture can be used to qualitatively describe the energy spectra of the particles produced. In an annihilation event where both a proton and an antiproton are at rest, the total energy available is twice the rest energy of the proton, a total of 1876.5 MeV. Assuming that at the instant of annihilation, this energy is shared equally (i.e., equipartitioned) among an average of five pions, the mean of the total energy awarded to each would be 375.3 MeV. A charged pion has a rest energy of 139.6 MeV so that in this simplified picture each has an average kinetic energy of 235.7 MeV. The situation is somewhat different for the neutral pions. The mean life of the π^o is extremely short, only 8.4 x 10^{-17} s. Therefore, at their mean kinetic energy, these particles travel only an average distance of 65.1 nm before decaying. The most prominent decay branch by far (98.8 %), is into two photons. In this simple picture an average of four photons with a mean energy of 187.6 MeV are produced in each annihilation event. Thus the radiation field is comprised of two components, an electromagnetic part due to the photons from the neutral pions and a hadronic part due to the charged pions. It is clear that these annihilations occurring "at rest" produce particles of rather high kinetic energies.

Since the pions as well as the decay photons have integer spin, they are classified as *bosons* and hence their natural statistical mechanical distribution in a "fireball" picture is the Bose-Einstein function, which for the massless photons is:

$$N_\gamma(E_\gamma) = \frac{C_\gamma E_\gamma^{\,2}}{\exp(E_\gamma / kT_\gamma) - 1}. \qquad (1)$$

$N_\gamma(E_\gamma)$ is the number of photons having energy E_γ per unit energy and the product, kT_γ, represents the product of Boltzmann's constant, k, and the absolute "temperature", T, in a statistical mechanical picture (for example, Tolman 1938). The product kT is conventionally measured in

MeV. A value of kT_γ of 69.5 MeV was found to result in a spectrum for which the average value of E_γ matched that calculated above while a value of C_γ of 1.242 x 10^{-6} MeV^{-3} was found to achieve the average total yield of 4.0 photons per annihilation. Others have reported the use of a Monte Carlo generated spectrum for these photons in order to subtract backgrounds in particle physics experiments (e.g., Graf et al. 1991). These spectra are compared in Fig. 1 and are similar in shape to that employed by Howe et al. (1988).

A spectrum for the charged pions can be generated similarly. For these particles of non-zero rest mass, this takes the more general form:

$$N_\pi(E_\pi) = \frac{C_\pi p_\pi W_\pi}{\exp(W_\pi / kT_\pi) - 1}. \qquad (2)$$

$N_\pi(E_\pi)$ is the number of charged pions of either sign having kinetic energy E_π per unit energy, p_π is the momentum, and W_π is the total relativistic energy given by $E_\pi + m_\pi$, with m_π denoting the rest energy of the charged pion. The relativistic form is needed since the kinetic energies of the pions are comparable with their rest energy. A value of C_π of 4.998 x 10^{-7} MeV^{-3} was found to achieve a total yield of 3.0 charged pions per annihilation and a value of kT_π of 110.0 MeV reproduced the average charged pion kinetic energy discussed above in this qualitative picture[†]. Reported experimental energy or momentum spectra for these charged pions are fragmentary at best. These have largely been measured for background subtraction purposes in experiments studying rare processes and commonly appear to reflect significant instrumental threshold effects. In Fig. 2, two examples of measured spectra (Gregory et al. 1976 and Angelopoulos et al. 1986) are compared with the spectrum calculated using eqn (2). The spectrum generated by eqn (2) is similar in shape to that used by Howe et al. (1988).

Antiproton annihilations in a Penning trap

If antiprotons at near rest energy are stored in a Penning trap or similar device for a long period of time (e.g., months), appreciable annihilations cannot occur on an ongoing basis without depleting the inventory. Thus, the intensity of steady-state prompt radiation near such a device will be at or near zero. Any prompt radiation is a result of a planned or unplanned event that terminates the storage. The principal terminating mechanisms, either accidental or intentional, are the loss or modification of the electromagnetic field perhaps due to a loss of electrical power, a breakdown in the cryogenic cooling of a superconducting magnet, or a failure to maintain vacuum in the device. Should the electromagnetic fields in the trap fail to continue to maintain the orbits of the antiprotons, the particles will annihilate through interactions with the materials comprising the trap. Alternatively, the failure of the vacuum results in annihilation by the antiprotons interacting with air. In either scenario, the resultant radiation is emitted in a nearly instantaneous "accident" and the hazard is that of the total acute dose equivalent.

Given the momenta of the charged particles released in such annihilations, the comparatively small electromagnetic fields used to contain the low momentum trapped antiprotons will produce inconsequential deflections of the charged particles of much higher momentum released in these events. Recognizing the modest dimensions of practical Penning traps, an isotropic point source approximation may be a reasonable one.

Radiation field produced by antiproton-nucleus annihilations

Thus, to quantitatively study the radiation fields produced by the annihilations that might occur in a Penning trap, antiproton-nucleus annihilations at near rest energy must be considered. One can follow the Monte Carlo algorithm of the MARS14 code by Mokhov (1995) as described

by Mokhov et al. (1998). Stopped antiprotons attach to nuclei in the same way as negative pions and muons. Annihilation at rest is assumed to produce only pions, neglecting some of the more rare modes involving strange particles. The charge distribution of the pions produced is slightly skewed towards negative pions in view of the "brought in" negative charge. Pion momenta are chosen from an inclusive distribution loosely based on experimental data. The energy-weighted distribution is normalized to twice the nucleon mass. This predicts a multiplicity of 4.3, a value close to that observed. In a complex nucleus the annihilation is treated as though it occurs on a free nucleon except that each pion produced by the annihilation process is given a 50 per cent probability to interact within the nucleus. This is intended to incorporate participation by the constituent nucleons. Nuclear target effects are approximated by allowing emerging particles to interact in the same nucleus or escape each with one half probability. Also added is a third component in which the antiprotons interact only quasi-elastically with the nucleons. These interactions can result in the release of nucleons, pions, and photons. The neutral pions, as discussed above, immediately decay into energetic photons that induce electromagnetic showers.

Although this algorithm describes all the main features of antiproton-nucleus annihilation, in the work reported in it was decided to use instead the state-of-the-art LAQGSM code by Gudima et al. (2001) based on the Quark-Gluon String Model. This was linked with the MARS14 code for the first time to do the calculations reported here. LAQGSM combines the intranuclear cascade model with the other models for the corresponding stages of nuclear interactions: quark-gluon string model, coalescence model, Fermi break-up model, and preequilibrium and evaporation models. Using the LAQGSM/MARS14 link, the emission fluences and spectra of various particles from the site of the annihilations were calculated. To utilize the code combination as it is presently written, it was necessary to artificially assign the

antiprotons a small, but finite kinetic energy of 0.5 MeV. Two different materials were studied; stainless steel representative of the materials comprising the trap and its walls (presumed to be magnetic materials, copper conductors, and the vacuum vessel) and air. The former is an attempt to deal with failures of confining orbits while the latter represents vacuum failures. Figs. 3 and 4 show the normalized energy spectra of the various particles produced by the antiproton-nucleus annihilations with these two selected materials. Table 1 provides a summary of the average numbers, $<N>$, and average energies, $<E>$, of the various particles produced in these annihilations. Included in this table are the results for protons, neutrons, pions (all three charges states), kaons (both charge states), photons produced directly (not resulting from π^o-decay), electrons (both charge states), and antiprotons.

Inspection of these results indicates that except for the photons for energies less than about 100 MeV, the differences between the two materials are not dramatic. However, the more energetic nucleons (neutrons and protons) produced by the annihilations in air are more important from a shielding standpoint. It is clear that nuclear effects in these annihilations are quite important, in particular with respect to the copious production of energetic nucleons. Thus, the annihilations in air form the "source term" for the shielding studies. The results for air are also likely to be representative of annihilations occurring in insulating materials such as plastics that might be used in a Penning trap.

Using these results as a source, the MARS14 code system was used to model the shielding of a conceptual Penning trap. The goal of these calculations was to design a shield to reduce the dose equivalent due to the loss of confinement of 10^{12} antiprotons to a level of approximately 0.05 mSv. A cylindrically symmetric geometrical configuration was used. The annihilations were modeled to occur within a spherical trap of 3 cm radius comprised of air

contained within a 2 mm stainless steel wall. Using standard cylindrical coordinates, an air cavern 200 cm long (-100 < Z < 100 cm) and 100 cm in radius (R < 100 cm) was set up around the trap that was located at the origin of coordinates. Following some preliminary runs of the code, two alternative shielding configurations were chosen as candidates for achieving the desired goal and were studied in high statistics calculations. **Shielding-A** is made of ordinary concrete while **Shielding-B** is comprised of iron followed with an outer layer of concrete. The outer layer of concrete for the latter is motivated by the well-known inability of a pure iron shield to adequately attenuate neutrons having energies slightly below 1 MeV (Alsmiller and Barish 1971; Elwyn and Cossairt 1986). The details of these cylindrical shields surrounding the air cavern described above are:

Shielding-A: ordinary concrete (ρ = 2.35 g cm^{-2}) at 100 < R < 400 cm, -400 < Z < -100 cm, 100 < Z < 400 cm.

Shielding-B: iron (ρ = 7.87 g cm^{-2}) at 100 < R < 240 cm, -240 < Z < -100 cm, 100 < Z < 240 cm, ordinary concrete ((ρ = 2.35 g cm^{-2}) at 240 < R < 280 cm, -280 < Z < -240 cm, 240 < Z < 280cm.

RESULTS AND DISCUSSION

Following the development of this preliminary design, high statistics Monte Carlo calculations were carried out as described. Fig. 5 is an illustration showing individual particle tracks followed in the Monte Carlo calculation for **Shielding-B** within that particular geometric configuration. Fig. 6 shows the resulting dose equivalent isocontours in **Shielding-A** normalized

to 10^{12} antiproton annihilations on air in the trap. Fig. 7 provides plots of the dose equivalent as a function of the coordinates *R* and *Z* within the two shielding configurations selected for detailed study, also normalized to 10^{12} antiproton annihilations. It is seen that the radial and axial dependences of the dose equivalent with distance in the shield are almost identical. This indicates that a spherical shield configuration, as intuitively expected, would perhaps be optimal. The slopes of the attenuation curves are qualitatively consistent with those encountered in other shielding problems involving hadrons of these energies. These two shielding configurations achieved their goals of 0.05 mSv in the postulated loss of antiprotons. In fact, **Shielding-B** would have met this goal with a slightly thinner shield. Certainly, **Shielding-B** is the more compact of the two shields. However these shields are large and rather massive with **Shielding-A** and **Shielding-B** having masses of 930 and 754 tonnes, respectively.

Obviously, 10^{12} antiprotons in storage in a Penning trap represents a quantity not yet achieved. For situations where a different number of antiprotons are trapped, the present results could be scaled to obtain an estimate the amount of shielding that might be needed to achieve a given dose equivalent rate at the exterior surface of the shielding. These results can also be used to estimate the radiation hazard of an unshielded Penning trap by using the ordinate-intercepts of these shielding curves along with an inverse square law dependence upon the distance from the source if the dimensions of the trap are small compared with the overall shield dimensions. In doing this, the practitioner should be careful to note that values of these ordinate-intercepts are not identical, reflective of the shielding material used.

CONCLUSION

The radiation fields produced by antiproton-nucleon annihilations at near rest energies have been described in a simple picture. It is clear that when large quantities of antiprotons are stored, the radiological hazards must be addressed and to do this properly, full scale high statistics Monte Carlo calculations should be used to fully account for the particles released in antiproton-nucleus annihilations. For small quantities of antiprotons, the prompt radiation hazards are negligible. Standard shielding techniques can mitigate the hazard of the sudden loss of the antiprotons. Since these prompt radiation hazards are novel, the regulatory paradigm concerning transport and use of storage devices for these particles differs from the usual considerations that pertain to radioactive materials shipments or, for that matter, to other types of radiological activities and will require further discussion. The results in this paper may be useful in addressing these questions. Future work for actual installations should employ detailed shielding calculations appropriate to the actual configuration envisioned.

Acknowledgments-The authors have benefited greatly from helpful comments received from Drs. Alexander Elwyn and Kamran Vaziri. This work was supported by the U. S. Department of Energy under Contract No. DE-AC02-76CH03000.

REFERENCES

Alsmiller Jr. RG, Barish J. Shielding against theneutrons produced when 400 MeV electrons are incident on a thick copper target. Part Accel 5:155-159; 1973.

Amsler C, Myhrer F. Low energy antiproton physics. Ann Rev Nucl Part Sci 41: 219-267; 1991.

Amsler C. Proton-antiproton annihilation and meson spectroscopy with the Crystal Barrel. Rev Mod Phys 70:1293-1339; 1998.

Angelopoulos A, et al. Study of charged particle production in $p\bar{p}$ annihilations at rest. In: Antiproton 86. Proceedings of the VIIth European symposium on nucleon-antinucleon interactions. Charalambous S, Papastefanou C, Pavlopoulos P. eds. Singapore: World Scientific; 1986: 79-204.

Brown LS, Gabrielse G. Geonium theory: Physics of a single electron or ion in a Penning trap. Rev Mod Phys 58: 233-311; 1986.

Elwyn AJ, Cossairt JD. A study of neutron leakage through an Fe shield at an accelerator. Health Phys 51:723-735; 1986.

Eades J, Hartmann FJ. Forty years of antiprotons. Rev Mod Phys 71:373-419; 1999.

Gabrielse G, Fei X, Helmerson K, Rolston SL, Tjoelker R, Trainor TA, Kalinowsky H, Haas J, Kells W. First capture of antiprotons in a Penning trap: A kiloelectronvolt source. Phys Rev Lett 57:2504-2507; 1986.

Gabrielse G. Harvard University: Gabrielse Research Group; 2002. Available at: http://hussle.harvard.edu/~gabrielse/.

Graf NA, et al. Search for narrow states in the inclusive γ-ray spectra resulting from antiproton annihilations at rest in liquid hydrogen and deuterium. Phys Rev D44:1945-1961; 1991.

Gregory P, Mason P, Muirhead H, Warren G, Hamer CJ, Ekspong G, Carlsson R, Holmgren SO,

Nilsson S, Stenbacka R, Walk Ch. Search for single cluster formation in annihilation reactions. Nucl Phys B102:189-206; 1976.

Groom DE et al. Review of particle properties. Eur Phys Jour C15:1-878; 2000. Available at: http://pdg.lbl.gov/.

Gudima KK, Mashnik SG, Sierk AJ, User manual for the code LAQGSM. Los Alamos National Laboratory Report LA-UR-01-6804; 2001.

Howe SD, Hynes MV, Picklesimer A. Portable pbars, traps that travel. In: Antiproton science and technology. Proceedings of a RAND workshop, Santa Monica, CA, 6-9 October 1987. Singapore: World Scientific; 1988: 481-481. (Also available as Los Alamos National Laboratory Report LA-UR-88-737; 1988.)

Landau R. Meson spectroscopy at LEAR. Ann Rev Nucl Part Sci 46:351-393; 1996.

Mokhov NV, The MARS code system user's guide, Fermi National Accelerator Report FN-628; 1995. More recent information is provided in Mokhov NV, Krivosheev OE, MARS code status. In: Proceedings of the Monte Carlo 2000 Conference, Lisbon; 23-26 October 2000: 934. (Also available as Fermi National Accelerator Laboratory Report Fermilab-Conf-00/181; 2000 and at http://www-ap.fnal.gov/MARS/.)

Mokhov NV, Striganov SI, Van Ginneken A, Mashnik SG, Sierk AJ, Ranft J, MARS code developments. In: Proceedings of the fourth workshop on simulating accelerator radiation environments (SARE4) sponsored by Oak Ridge National Laboratory, Knoxville, TN; 14-16 September 1998: 87-99. (Also available as Fermi National Accelerator Report Fermilab-Conf-98/379; 1998.)

Pais A. The many π-meson problem. Ann of Phys 9:548-602; 1960.

Tolman RC. The principles of statistical mechanics. London: Oxford University Press; 1938.

Tseng CH, Gabrielse G. Portable trap carries particles 5000 kilometers. Hyperfine Inter 76: 381-386; 1993.

FOOTNOTE

†While the two values of *kT* were arbitrarily used to fit the spectra to the calculated average energies of photons and charged pions, their magnitudes are sensible if one naively assumes that the proton and antiproton overlap immediately prior to annihilation and that each of the five pions are localized within one fifth of a spherical volume having a 1.2 fm radius, a representative nucleon "size", immediately prior to the annihilation. Application of the Heisenberg uncertainty principle results in a pion momentum of 206 MeV/c and a kinetic energy of 108 MeV.

Table 1 Average multiplicities, $<N>$, and energies, $< E >$ (MeV), for protons, neutrons, pions, kaons, photons, electrons, and antiprotons emitted from antiproton annihilations in air and stainless steel as calculated using LAQGSM/MARS14.

	Air		**Stainless Steel**	
Particle	**<N>**	**<E>**	**<N>**	**<E>**
p	1.761	84.92	4.290	50.18
n	3.538	180.26	6.011	92.70
π^+	0.556	237.95	0.595	216.61
π^-	0.851	243.60	0.871	225.26
π^0	0.906	221.40	0.931	206.47
K^+	3.4×10^{-4}	72.04	1.2×10^{-3}	75.80
K^-	1.4×10^{-4}	49.41	3.3×10^{-4}	45.10
γ	0.137	307.96	0.126	336.14
e^-	9.4×10^{-4}	149.00	8.7×10^{-4}	165.82
e^+	7.9×10^{-4}	181.13	8.7×10^{-4}	210.50
$\overline{p}$	5.7×10^{-4}	0.27	1.4×10^{-4}	0.21

List of Figure Captions

1. Normalized Bose-Einstein photon energy spectrum and referenced Monte Carlo spectrum of Graf et al. (1991).
2. Normalized Bose-Einstein charged pion spectrum along with the Measured Spectrum 1 of Gregory et al. (1976) and Measured Spectrum 2 of Angelopoulos et al. (1986). The normalizations of the measured spectra are arbitrary.
3. Normalized energy spectra of pions and photons produced by antiproton-nucleus annihilations in air (top frame) and stainless steel (bottom frame).
4. Normalized energy spectra of protons (p) and neutrons (n) produced by antiproton-nucleus annihilations in air (top frame) and stainless steel (bottom frame).
5. MARS geometry model of **Shielding-B** with a sample of particle tracks resulting from antiproton annihilations on air in the trap as calculated by the LAQGSM/MARS Monte Carlo code combination.
6. Calculated dose equivalent isocontours in **Shielding-A** normalized to 10^{12} antiproton annihilations on air in the Penning trap volume. The maximum and minimum values found in this plot were $3.4 \times 10^{+5}$ and 6.1×10^{-4} mSv, respectively.
7. Plot of the calculated dose equivalent in **Shielding-A** (top frame) and **Shielding**-B (bottom frame) as a function of radial coordinate *R* (solid lines) and axial coordinate *Z* (dashed lines) at their maximum values for 10^{12} antiproton-nucleus annihilations in air within a 3 cm radius volume located at the origin of coordinates at the center of a cylindrical shield described in the text.

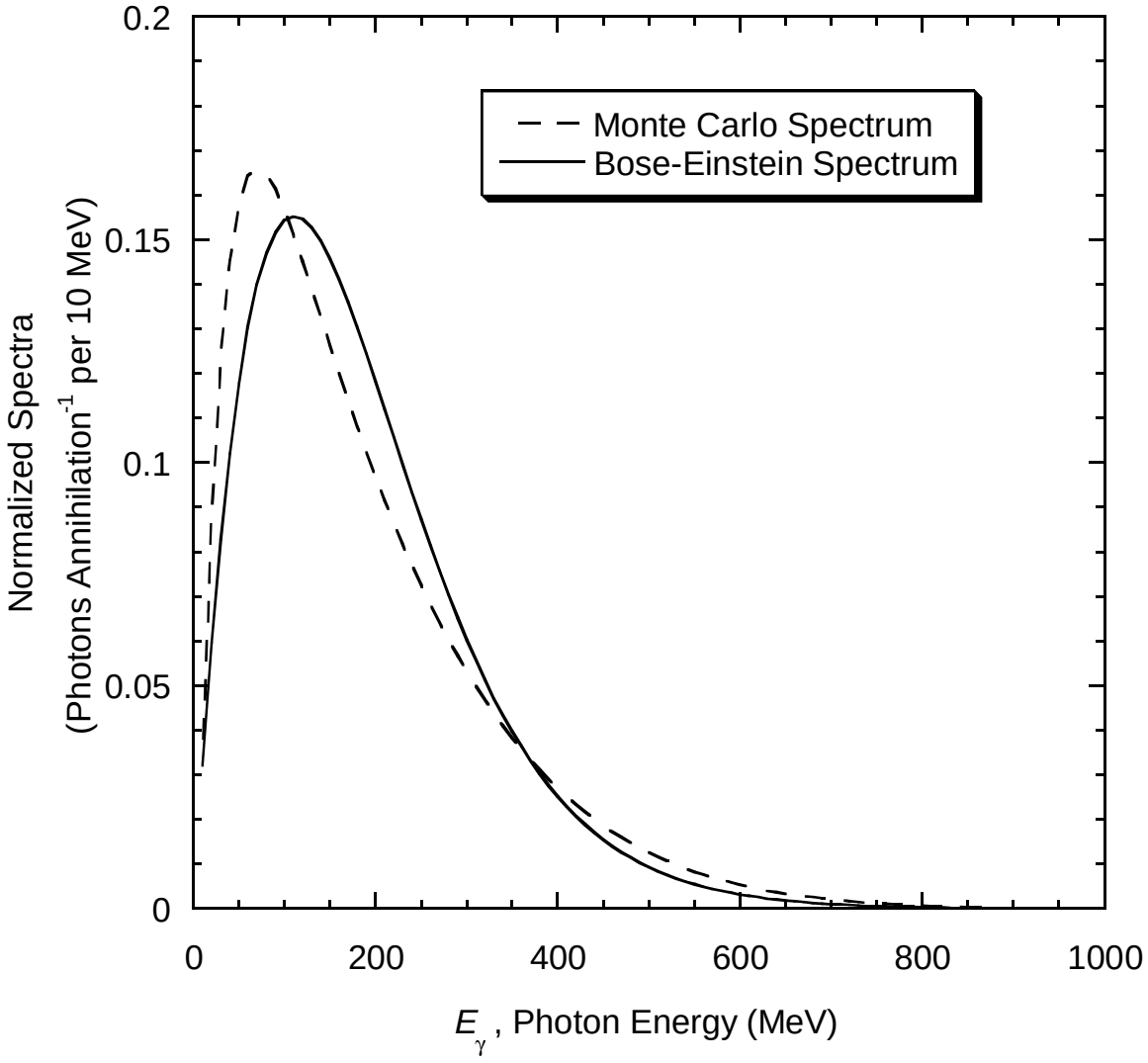
0.2
0.15
0.1
0.05
0
0
200
400
600
800
1000
Monte Carlo Spectrum
Bose-Einstein Spectrum
Normalized Spectra
(Photons Annihilation-1 per 10 MeV)
Eγ , Photon Energy (MeV)

Figure 1

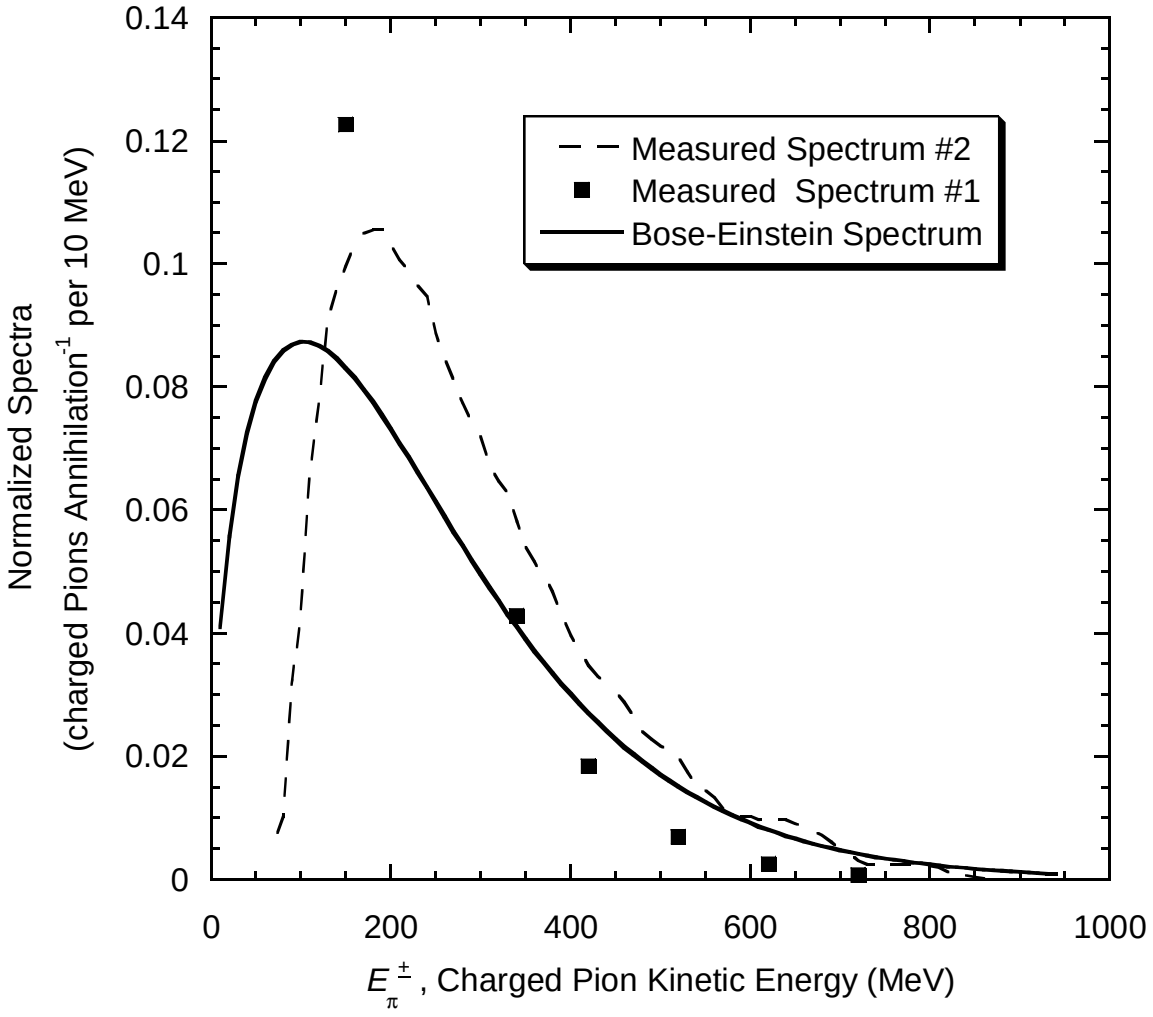
0.14
0.12
0.1
0.08
0.06
0.04
0.02
0
0
200
400
600
800
1000
Normalized Spectra
(charged Pions Annihilation-1 per 10 MeV)
Measured Spectrum #2
Measured Spectrum #1
Bose-Einstein Spectrum
E± π, Charged Pion Kinetic Energy (MeV)

Figure 2

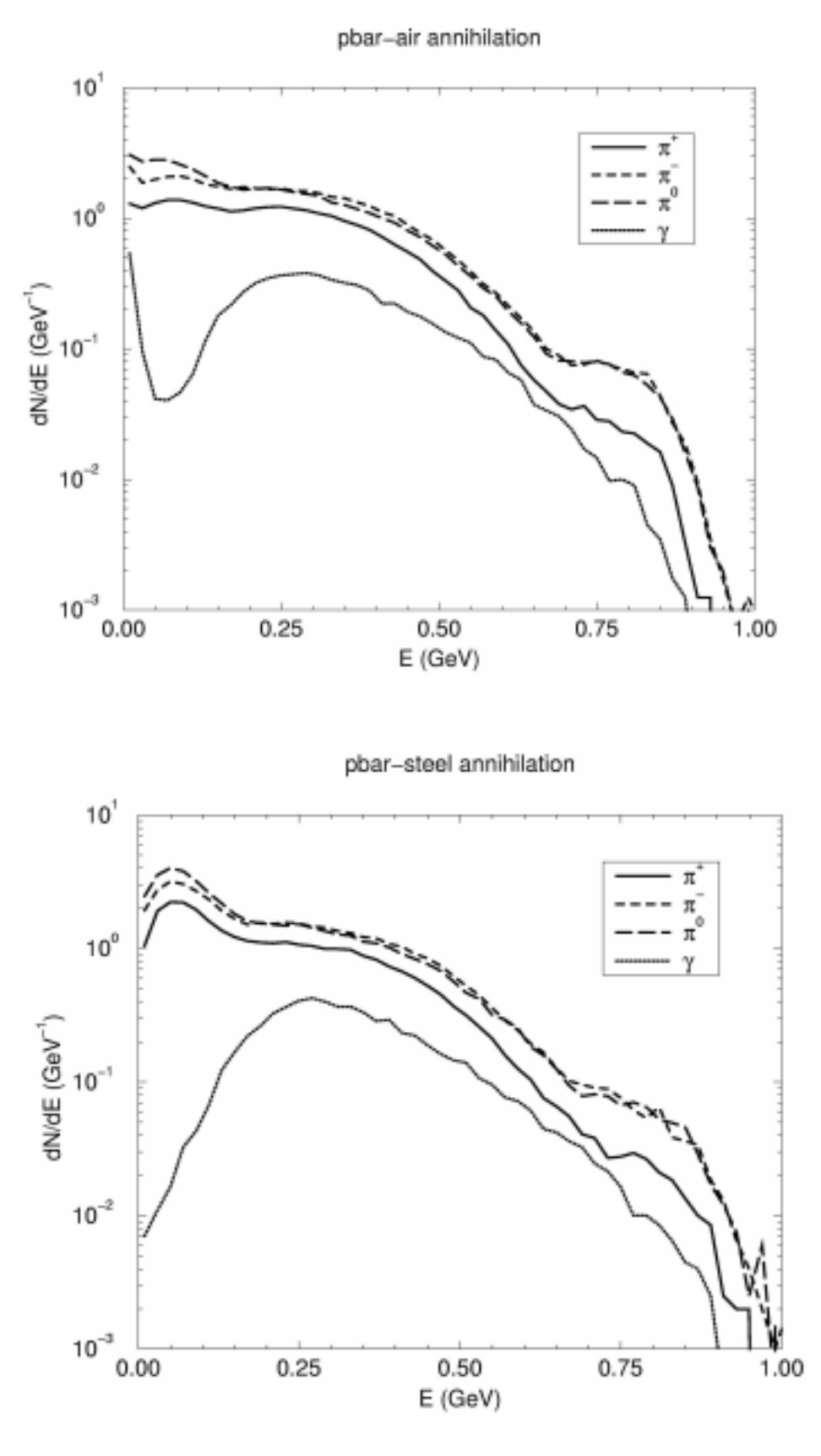
pbar–air annihilation
dN/dE (GeV⁻¹)
E (GeV)
π⁺
π⁻
π⁰
γ
pbar–steel annihilation
dN/dE (GeV⁻¹)
E (GeV)
π⁺
π⁻
π⁰
γ

Figure 3

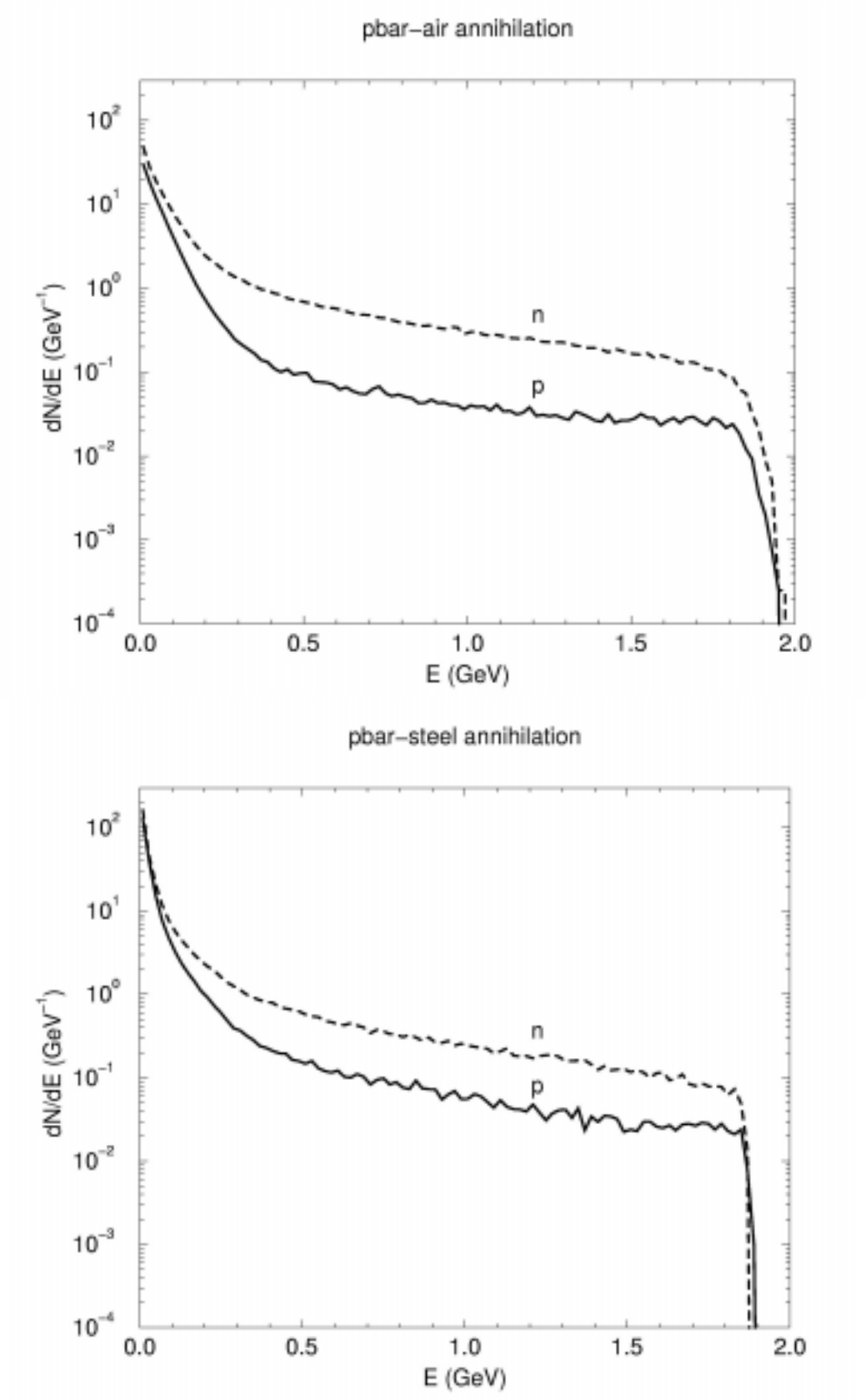
pbar–air annihilation
dN/dE (GeV⁻¹)
E (GeV)
n
p
pbar–steel annihilation
dN/dE (GeV⁻¹)
E (GeV)
n
p

Figure 4

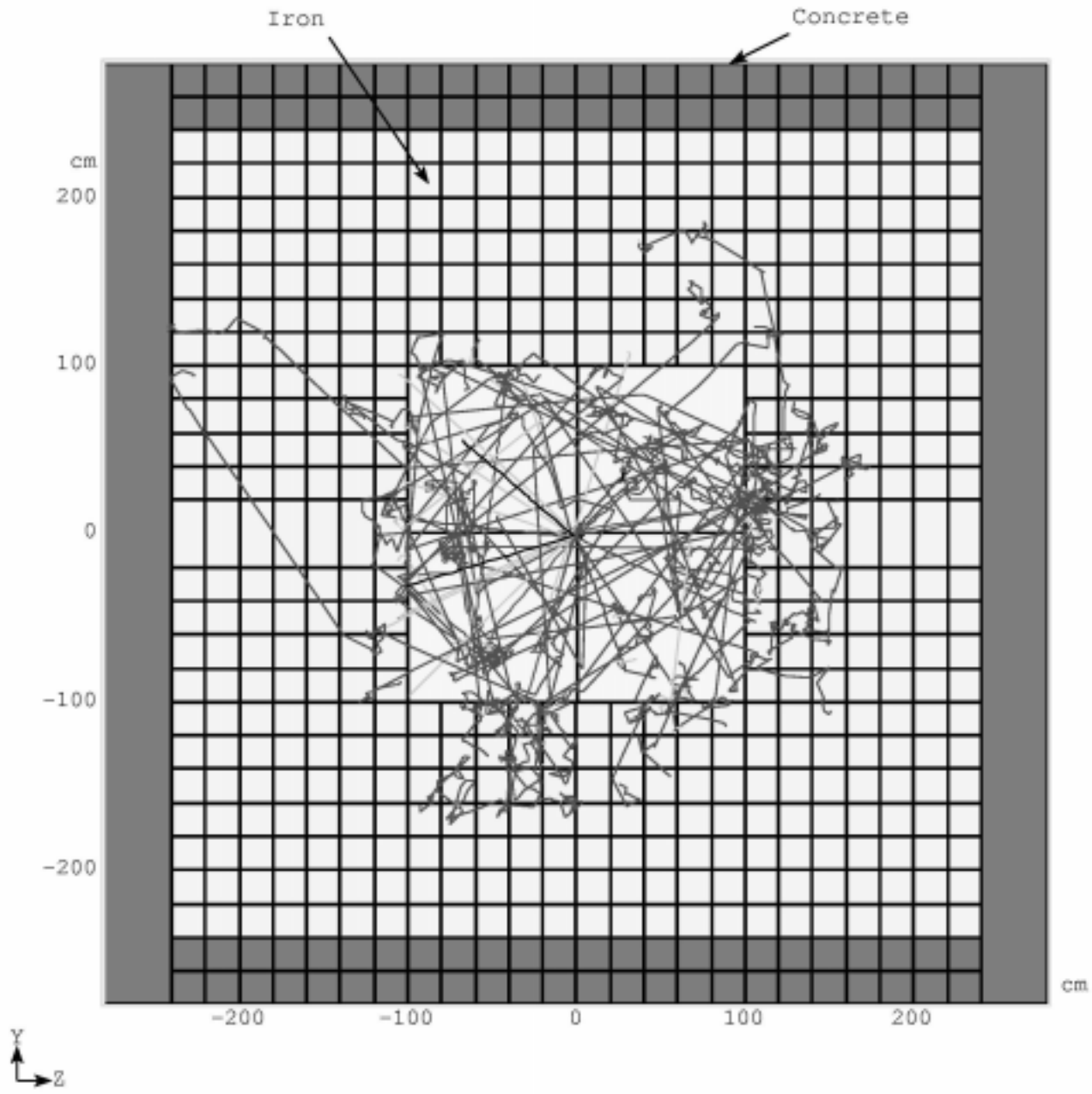

Figure 5

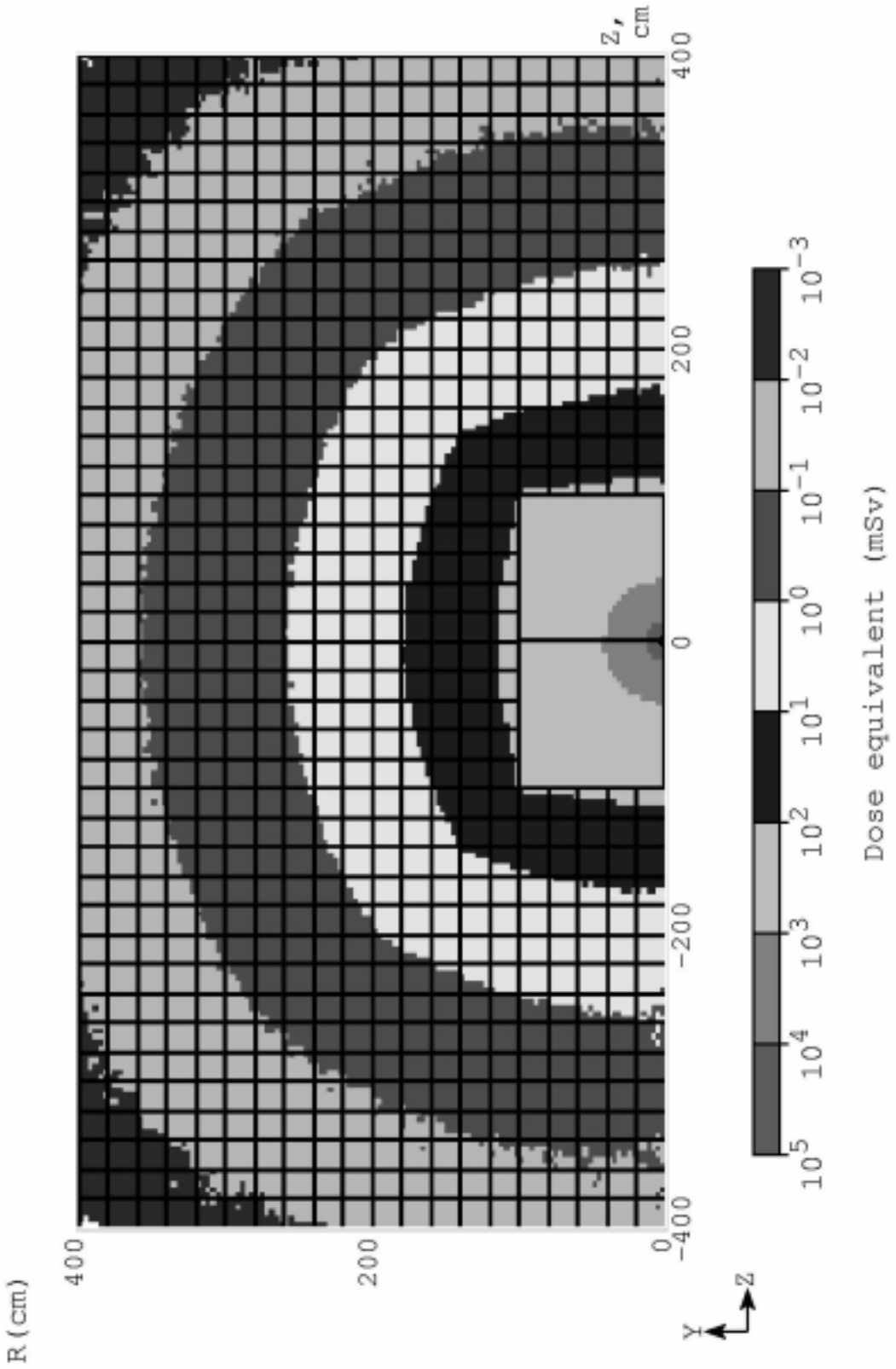
Z, cm
400
200
0
−200
−400
R (cm)
400
200
0
Y
Z
Dose equivalent (mSv)
10^{5}
10^{4}
10^{3}
10^{2}
10^{1}
10^{0}
10^{-1}
10^{-2}
10^{-3}

Figure 6

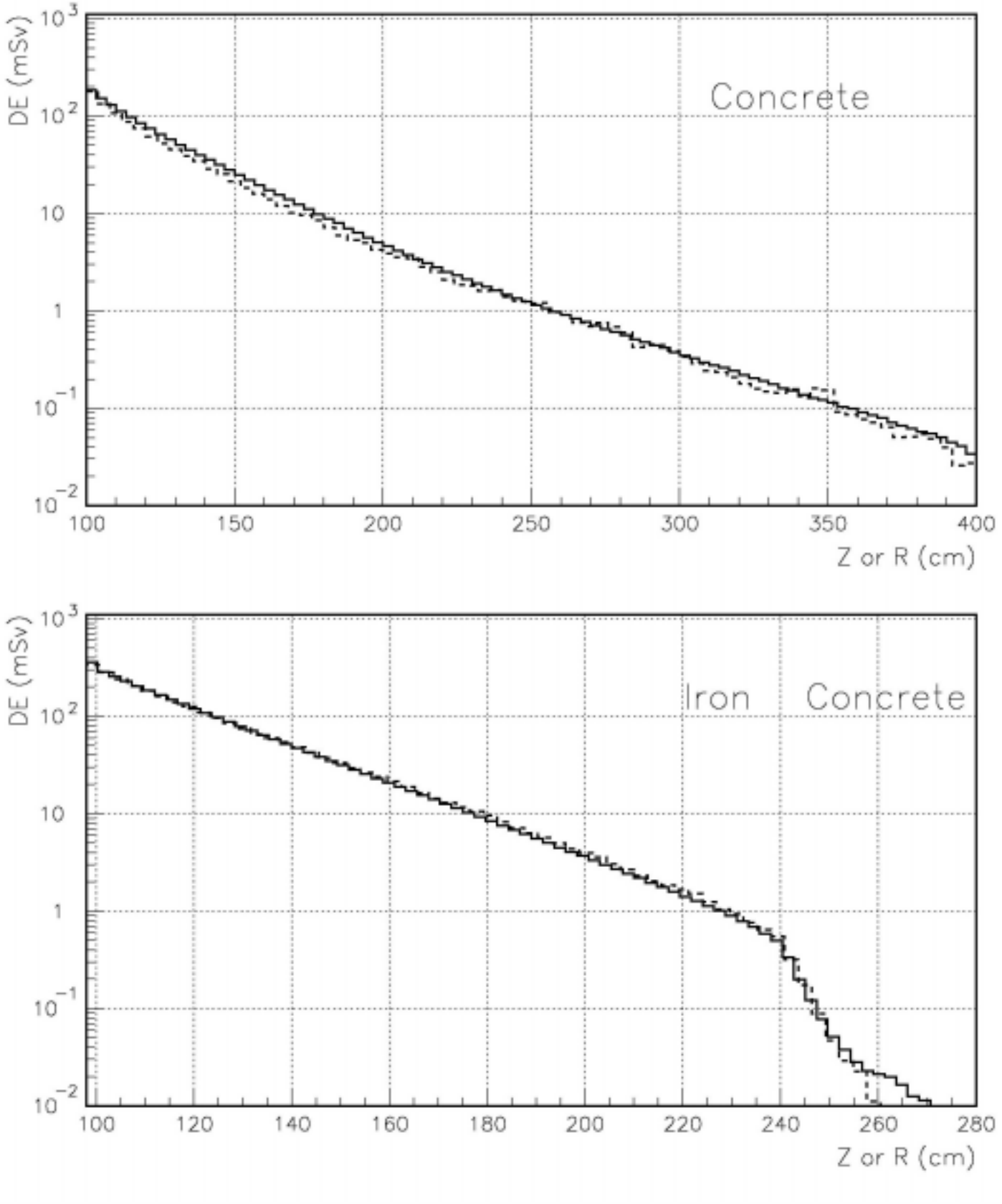

Figure 7